Natural roller bearing fault detection by angular measurement of true instantaneous angular speed

Laurence Renaudin, Frédéric Bonnardot, Olivier Musy, J.B. Doray, Didier Rémond

www.elsevier.com/locate/ymssp

Natural roller bearing fault detection by angular measurement of true instantaneous angular speed

L. Renaudin, F. Bonnardot, O. Musy, J.B. Doray, D. Rémond

PII: S0888-3270(10)00148-2
DOI: doi:10.1016/j.ymssp.2010.05.005
Reference: YMSSP 2583

To appear in: *Mechanical Systems and Signal*

Received date: 7 May 2010
Accepted date: 12 May 2010

Cite this article as: L. Renaudin, F. Bonnardot, O. Musy, J.B. Doray and D. Rémond, Natural roller bearing fault detection by angular measurement of true instantaneous angular speed, *Mechanical Systems and Signal*, doi:10.1016/j.ymssp.2010.05.005

Natural roller bearing fault detection by angular measurement of true instantaneous angular speed

L. Renaudin[1], F. Bonnardot[2], O. Musy[3], J.B. Doray[4], D. Rémond[1*]
[1] Université de Lyon, CNRS, UMR5259
INSA-Lyon, LaMCoS, F-69621, Villeurbanne, France
e-mail: **didier.remond@insa-lyon.fr**
[2] Université de Lyon,
Université Jean Monnet - IUT de Roanne, LASPI, F-42334, Roanne, France
[3] SNR Roulements
1, rue des usines, F-74000 Annecy
[4] VOLVO 3P
Renault Trucks SAS (API TER H50 1 22)
99, route de Lyon, F-69806, Saint-Priest Cedex, France

Abstract

The challenge in many production activities involving large mechanical devices like power transmissions consists in reducing the machine downtime, in managing repairs and in improving operating time. Most online monitoring systems are based on conventional vibration measurement devices for gear transmissions or bearings in mechanical components. In this paper, we propose an alternative way of bearing condition monitoring based on the instantaneous angular speed measurement. By the help of a large experimental investigation on two different applications, we prove that localized faults like pitting in bearing generate small angular speed fluctuations which are measurable with optical or magnetic encoders. We also emphasize the benefits of measuring instantaneous angular speed with the pulse timing method through an implicit angular sampling which ensures insensitivity to speed fluctuation. A wide range of operating conditions have been tested for the two applications with varying speed, load, external excitations, gear ratio, … The tests performed on an automotive gearbox or on actual operating vehicle wheels also establish the robustness of the proposed methodology. By the means of a conventional Fourier transform, angular frequency channels kinematically related to the fault periodicity show significant magnitude differences related to the damage severity. Sideband effects are evidently seen when the fault is located on rotating parts of the bearing due to load modulation. Additionally, slip effects are also suspected to be at the origin of enlargement of spectrum peaks in the case of double row bearings loaded in a pure radial direction.

Keywords

bearing; fault detection; instantaneous angular speed; angular sampling; encoder

1 Introduction

Numerous papers have focused on detection and diagnosis of faults in rolling element bearings with the expected goal to reduce downtime of machines, to manage repairs and improve their operating time. Conventional approaches are based on the assumption that effects of bearing faults can be considered as load fluctuations in time associated to impact of rolling elements when passing through the fault [1], [2], [3]. These load fluctuations induce excitation of structural resonances or displacements of shafts whose consequences are resulting vibrations which can be measured [4]. Classical Condition Monitoring Systems (CMS) take advantage of non intrusive transducers like accelerometers or electrical motor currents but they suffer from the transmission path between the excitation and the transducers [2].

From a data acquisition point of view, CMS traditionally use time sampling method (with constant time step) and analysis tools based on frequency investigations. As rolling element bearings present a discrete geometry in rotation, this kind of data acquisition implies that revolution speed has to be as constant as possible during the measurement. Even if the revolution speed is monitored, mechanical and electrical operating conditions induce small speed fluctuations [5]. These fluctuations generate frequency modulation on all the time sampled signals. Moreover, these established speed fluctuations act like modulating excitations on structural fixed resonances, leading to response signals with a very rich spectrum [6]. Moreover, the modulation effect is also renowned for the moving load in reference with the fault location [4]. All these modulation effects are directly related to the geometry and kinematic properties of the rolling element bearings. Several studies on monitoring geared systems have also shown similar effects [2, 10, 11]

Therefore, great research efforts have been concentrated on signal processing methods in order to extract valuable information and/or to cancel transfer functions of this transmission. Many different investigations have been carried out on this problem, introducing various analysis tools, based on either deterministic approaches like frequency demodulation [5, 7] or stochastic methods like cyclostationarity [8]. Generally, the efficiency of these remains dependent on operating conditions or linked to particular geometry architecture of machines under consideration.

An alternative methodology appeared two decades ago by measuring other effects of faults in geared systems like Transmission Error [9, 10, 11] involving new sensors like optical encoders [12]. In the meantime, the notion of instantaneous frequency appears and signal processing tools allow extracting valuable information for condition monitoring [13]. From turbo machines, order tracking is also investigated in order to adapt sampling frequency with revolution speed [14] but in the time domain. In the recent years, instantaneous angular speed becomes one of the most promising investigation way for monitoring geared mechanical systems [11, 15], internal combustion engines [16] or electrical motors [17]. Generally, acquisition of instantaneous angular speed is processed in the time domain or not precisely presented.

This paper stands essentially on a first experimental approach and suggests an alternative measurement approach for detecting local faults in rolling element bearings, particularly emerging pitting faults in outer or inner race. The main assumption made in this work assumes that very small revolution speed fluctuations are induced by the presence of local faults only by changes in the kinematics. This alternative way of detecting faults is based on instantaneous angular speed measurement by the help of optical or magnetic encoders. Nowadays, these transducers have been widely used for gear transmission characterisation and now reach an interesting level of maturity and integration in mechanical systems. The first section of the paper is devoted to the general presentation of angular speed measurement in the angular domain with encoders. The measurement principle applies the pulse timing method for high precision time location of encoder signal events. Then, the second section exhibits results obtained on an automotive transmission gearbox equipped both with optical and magnetic encoders. Different operating conditions have been investigated for three fault conditions on the outer race of a tapered roller bearing. More experimental results on automotive wheels are presented in the third section. Investigations are performed on double row tapered roller bearings with different kinds of actual and induced faults. Various

actual operating conditions have been examined systematically during tests. The last section presents some conclusions and perspectives for this promising way of fault detection in rolling element bearings.

2 Angular instantaneous revolution speed measurement

2.1 General considerations on bearing fault signature

Bearings in general consist of two concentric rings, outer and inner, with balls or rollers between them (Fig 1). The balls are bound by a cage which ensures a uniform distance between them and prevents any contact during revolution. The bearings can be damaged by external causes like contamination of the bearing by external particles (dust or sand), like corrosion induced by the penetration of water, acids, inadequate lubrication which can cause heating and the wear of the bearing, bad alignment of the shafts, current which crosses the bearing and which causes electric arcs.

Bearing defects can occur because of metal fatigue under normal operational conditions. Generally, cracks will appear on the tracks or/and on the balls. Then, chipping and tearing off of material induce initial spalls and can quickly accelerate the wear of a bearing. In the first stage of this material removal, load or speed fluctuations due to the repetitive impacts of the moving components on the defect are diffuse but they grow as faults spread along the contact surface. For instance, when a rolling element contacts a defect on the inner or outer raceway, it produces a variation in load or in kinematics which is sudden and local at the beginning of this wear process and becomes extended when the damage covers a large area of the contact surface.

In an operating bearing, a series of impacts occurs with a repetition frequency which depends on whether the defect is on the inner, on the outer race, or on the rolling element. Therefore, the overall phenomenon signals measured on the bearing show a periodic pattern. The defect will produce one of the four characteristic fault frequencies depending on which bearing surface contains the fault. Each bearing defect has its own signature and it is characterized by a well-known frequency which can be calculated starting from the geometry and dimensions of the bearing (See equations (1)-(4) and Figure 1).

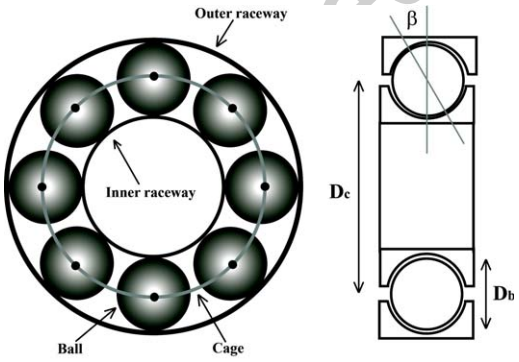

D_B = ball diameter

D_C = pitch diameter

N_B = number of rolling elements

β = ball contact angle

F_R = rotating shaft frequency

Figure 1: Structure and main dimensions of a roller bearing

$$\text{cage fault frequency}: \; F_C = \frac{1}{2}\left(1 - \frac{D_B}{D_C} \cdot cos\,\beta\right) F_R \tag{1}$$

$$\text{inner race fault frequency}: \; F_I = \frac{N_B}{2}\left(1 + \frac{D_B}{D_C} \cdot cos\,\beta\right) F_R \tag{2}$$

$$\text{outer race fault frequency}: F_O = \frac{N_B}{2}\left(1-\frac{D_B}{D_C}\cdot cos\,\beta\right)F_R \quad (3)$$

$$\text{ball fault frequency}: F_B = \frac{D_C}{D_B}\left(1-\left(\frac{D_B}{D_C}\cdot cos\,\beta\right)^2\right)F_R \quad (4)$$

In the case of vibration signal, this pattern consists in a succession of oscillating bursts dominated by the major resonance frequency of the structure defined by the bearing and its support. Furthermore, when the position of the defect is moving with respect to the load distribution on the bearing, the series of impacts is modulated in amplitude. From these considerations, some randomness should be expected in the measured vibration signal as well as some amplitude modulation.

As pointed out in literature, rolling element bearings can experience some slip of the rolling elements which can induce either constant or random deviations in frequency location estimated from the kinematics. The constant component in this difference is commonly attributed to the actual dimensions of the bearing compared to the nominal dimensions, and to mean load which induces deformations and mean placement of rolling elements. For example, if taper roller bearings are considered, the bearing geometry induces slip between the rollers and the races except at one axial position which can vary with load, alignment, etc. The random component can be associated with the random placement of each rolling element at the time of each impact. Therefore, this phenomenon leads to a spread of frequency location associated with local changes in kinematics. As a consequence, this yields to the fact that occurrences of the impacts never reproduce exactly at the same position from one cycle to another.

In this study, all the defects are located on the fixed part of the bearing, either on the inner or the outer races of the bearing, leading to a non moving load condition. Moreover, it is also assumed that random slip of rolling elements is negligible and frequencies are approximately located by equations (1)-(4) in reference to the rotation frequency of the shaft, with low differences due to load or actual kinematics.

2.2 Revolution speed measurement and angular sampling

Revolution speed measurements are carried out by using through shaft encoders directly mounted on the shaft of interest. These transducers deliver square form signals as gratings on a disc pass in front of a sensitive detector. Gratings can be geometrical notches with proximity transducers, magnetic patterns in the case of magnetic encoders or optical patterns with light sensitive transducers. Noisy sine signals delivered by raw transducers are generally processed electronically to provide TTL signal, including interpolating features. Therefore, resolution of encoders is given by the resolution of the coding element and by the interpolating factor. All these processing procedures can be embedded in the encoders and introduce signal distortions defining the global precision and quality of the transducer. Generally speaking, optical encoders are the highest precision transducers even if magnetic encoders reach now sufficient precision for precision rotation speed measurements.

Revolution speed measurement is performed with the help of the Pulse Timing Method largely used in gear Transmission Error measurement. The instantaneous angular speed is estimated for each pulse of the encoder signal by counting pulses delivered by a high frequency clock as presented in Figure 2. The data acquisition system consists of a high frequency counter device which can be commonly found on traditional data acquisition board. The angular speed is given by the following equation (5) and depends only on the resolution of encoder (N) and on the clock frequency (f_H).

$$\varpi_i = \frac{2\pi}{N}\cdot\frac{f_H}{N_i}\ (\text{rad.s}^{-1}) \quad (5)$$

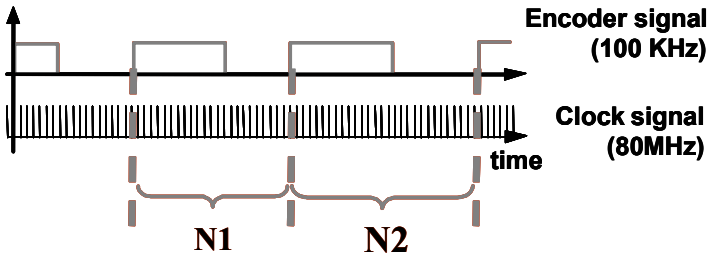

Figure 2: Principle of pulse timing method involved in instantaneous speed measurement

The acquisition process is equivalent to having time estimation N_i between successive rising edges of the encoder signal and this for each of them. Therefore, the acquisition occurs at a sampling rate directly linked to the shaft rotation speed (and of course to the resolution of the encoder). It is more convenient to keep angular sampling and not to come back to the time domain because this transformation implies sampling modulations associated to revolution speed fluctuations.

As only revolution speed fluctuation are of interest in this study, all the signal processing and analysis performed in this paper will be done not on the instantaneous angular speed ϖ_i but on the time duration N_i of successive encoder gratings.

2.3 Frequency location of bearing faults with angular sampling

If acquired signals are sampled in the angular domain of the rotating shaft position, all the bearing frequencies are generally exactly located at a non integer multiple of the shaft frequency. Performing an FFT on angular sampled signals leads to a spectral energy expansion on order components in reference to shaft revolution. Any phenomenon which appears α-times periodically during one revolution of the shaft will be expanded on the component located at frequency of α order. Then, each specific frequency of rolling element bearing is perfectly located in angular frequency domain. For example, in the case of an outer race fault, the FFT of any signal sampled in the angular domain should present a significant component at the α order corresponding to the ratio of the outer race frequency over the rotating shaft frequency. This angular frequency component generalizes the conventional order analysis with non integer orders and is related to the bearing kinematics by :

$$\alpha = \frac{N_B}{2}\left(1 - \frac{D_B}{D_C}\cdot cos\,\beta\right) \tag{6}$$

This ratio can also be interpreted as the number of events (speed fluctuation due to kinematic changes introduced by a spall) which occur during one revolution of the shaft.

Another key advantage of angular sampling is given by the accuracy of frequency separation which can be reached. Indeed, in order to increase the number of frequency channels, the signal length on which the FFT is performed must be as large as possible. When time sampling is used, rotation speed fluctuations induce the spread of a particular frequency component on channels close to the target one. When angular sampling is performed on signals, no modification due to rotation speed fluctuations occurs and frequency components related to specific angular periodicity are already attached to the same angular frequency channel. Therefore, angular sampling makes it possible to Fourier Transform very large signals, giving access to high resolution spectral analysis and to the capability of sorting very low and close magnitude components. Moreover, this important key feature opens the opportunity to perform measurement under varying speed operating conditions, avoiding constant speed requirements generally laid down when time sampling is performed.

3 Experimental results on automotive gearbox test bench

3.1 Description of the test bench and signal processing

The test bench dedicated to this study is made up of an automotive gearbox, driven by an electrical motor mounted in an open loop design allowing generation of an acyclic excitation. The gearbox is loaded by the help of an electrical generator which is torque monitored. Revolution speed of the whole kinematic chain can be controlled over a large range of operating conditions. The gearbox presents a first reduction stage with four different gear ratios and a second stage with 64/15 gear ratio. Only two gear ratio conditions have been investigated (3rd with a 27/31 gear ratio and 4th with 45/37 gear ratio).

The gearbox is equipped with different transducers on the two main shafts as shown in Figure 3. Optical encoders offering through shaft design and 2048 pulses per revolution are mounted on a plate close to the faulty bearing.

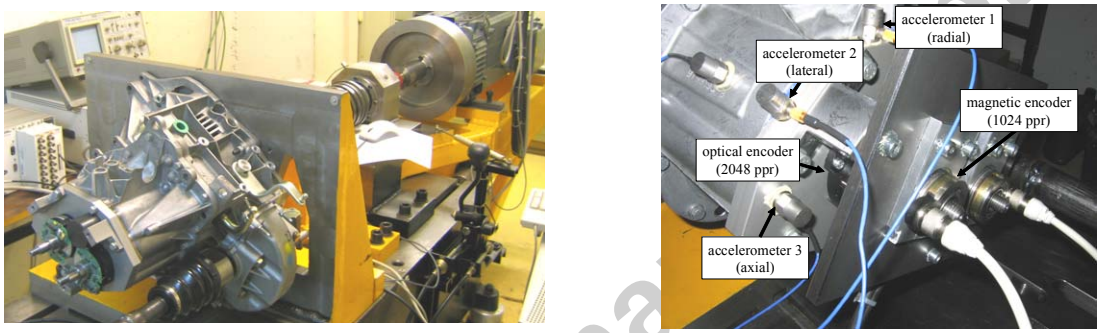

(a) overall view of the test bench with electrical motor in the background

(b) transducers location on the gearbox

Figure 3: Test bench overview showing gearbox and its transducers

Magnetic encoders (SNR SLE XAB-41072) are included in an integrated design with roller bearing and these are located at the free end of shafts with a second plate. In this test application these bearings are not functional bearings but are only used as added encoders. The resolution of these encoders reaches 1024 pulses per revolution by increasing raw resolution of the magnetic pattern (32 pairs of magnetic poles) by an interpolation factor. Accelerometers are also available as classical transducers but are not used in this experimental campaign.

The defective bearing on this gearbox is a tapered roller bearing (SNR 32005) with 17 rolling elements. All the main characteristics of this bearing are reported in Table 1. From writing velocity relationships between bearing elements, the frequency location of an outer race fault can be estimated by equation (7). With numerical values, this leads to the frequency of an outer race fault being located at 7.2521 times the rotation frequency of the supported shaft.

$$F_O = \frac{N_B}{2} \cdot \frac{sin(\kappa - \varepsilon)}{sin(\kappa).cos(\varepsilon)} \cdot F_R \tag{7}$$

Geometrical characteristics	Value for SNR 32005
Number of rolling elements (N_B)	17
Inclination angle of rolling element axis (κ)	13°55’
Half-cone angle of rolling element (ε)	2°05’

Table 1: Main geometrical dimensions for tapered roller bearing

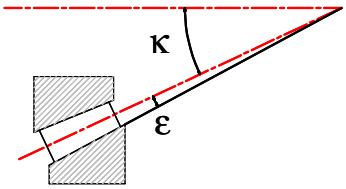

Figure 4: Geometric angle definition for tapered rolling bearing

Three different levels (without, small and large fault) of natural and actual pitting faults are considered in this paper. For confidential reasons, only a qualitative description of these faults is summarized in Figure 5. The orientation of the outer race in the casing is set for the load applied on the bearing to be in the direction of fault location.

(a) outer race orientation and fault location (large spall)

(b) actual pitting fault shape defined as small spall

Figure 5: Fault description and location on the outer race

Signal processing consists of a simple Fourier Transform of the signal representing the time intervals between pulses of the encoder. In order to have sufficient spectral resolution, this analysis is performed on large signals corresponding to 353 shaft revolutions with optical encoders (722 944 points) and 450 revolutions for magnetic encoders (460 800 points). The FFT is calculated without any normalization for the length of the signals therefore limiting the possibility to compare signals only for each kind of transducers. As for all operating conditions the length of signals is kept the same, comparison between these measurements can be done but remains relative.

Various operating conditions in torque and speed have been investigated in this study but only some of them are presented in the next section for constant or varying operating speed.

3.2 Measurements with constant speed operating conditions

In this section, results of measurements carried out for constant rotation speed of the supported shaft (300 rpm) and for constant applied torque (60 Nm) are presented in the case where the 4th gear is engaged.

3.2.1 Measurements with optical encoders

In Figure 6, the three different outer races have been tested and the figure shows the main spectral components.

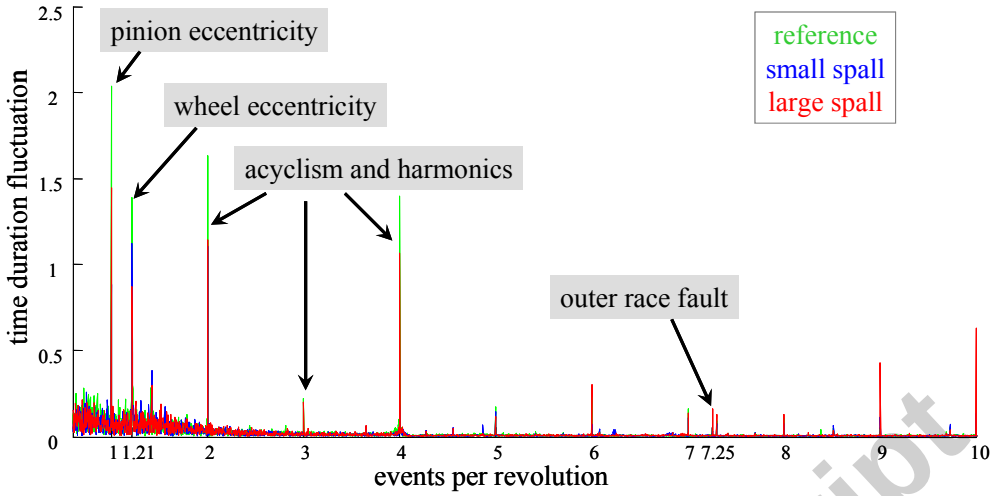

Figure 6: Instantaneous angular speed spectra of angular sampled signal of pulse time duration with optical encoder

First of all, the main gear frequencies are obviously visible and located at the primary shaft rotation frequency due to eccentricity of the pinion (order 1), at the gear ratio order for eccentricity of the wheel (order 1.2162), and at integer orders for acyclism and harmonics. As expected, the component at angular frequency corresponding to 7.2521 events per revolution appears in the spectrum, particularly for the large spall conditions. A magnification of the bandwidth from order 7.2 to order 7.4 presented in Figure 7 shows that component due to outer race fault increases as the size of the spall increases.

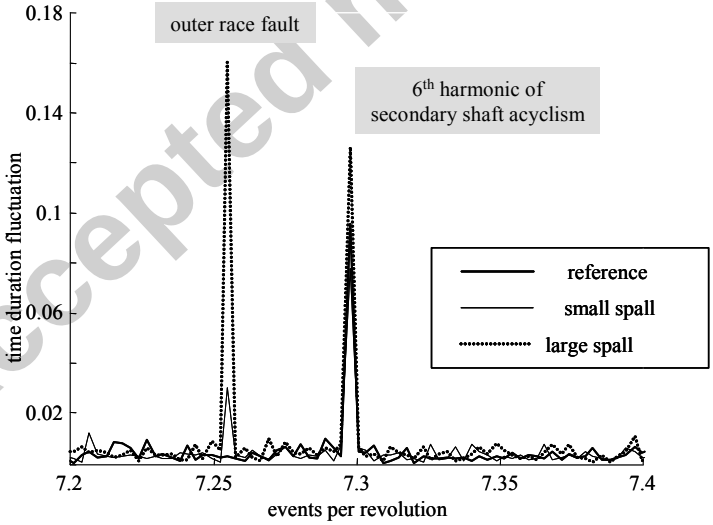

Figure 7: Focused view of the instantaneous speed spectra

In the reference condition without spall, the level of the target frequency channel is null while it takes a significant level when the spall is large. The frequency channel located at 7.2972 just near the target frequency has rather the same level for the three operating conditions. This component has been found to be associated with the 6th harmonic of secondary shaft acyclism.

In order to demonstrate this assumption, some additional tests have been performed with the 3rd gear engaged. With this new condition, the component should appear at angular frequency order 5.2258. The Figure 8 shows the focused bandwidths for the two gear conditions in presence of a large outer race spall

with the acyclism component moving from 7.2972 frequency channel to 5.2258. Another important conclusion of this comparison is given by the fact that the level of the targeted channel remains constant even if the gear conditions are changed and from one measurement to the other, proving the robustness of the proposed approach.

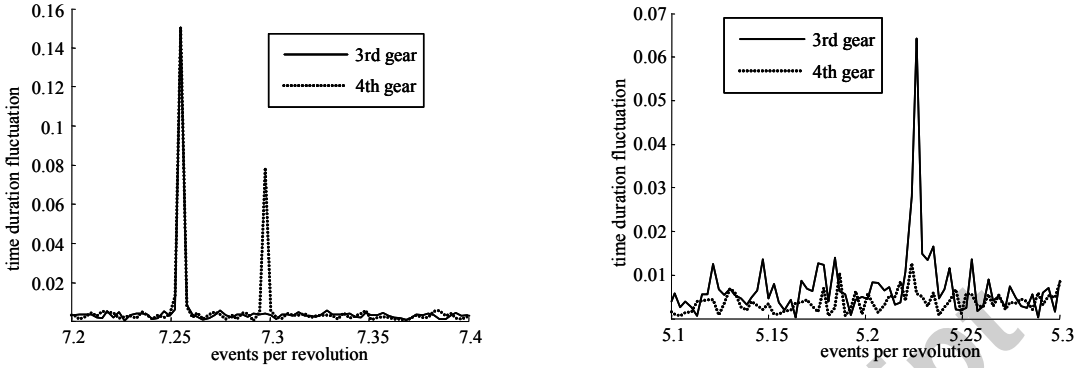

(a) focus around outer race fault frequency

(b) focus around 6th harmonic of secondary shaft acyclism

Figure 8: Difference recorded on instantaneous angular speed spectra for two gear ratios

Moreover, a fault component like acyclism harmonic can be monitored with an encoder either mounted on the target shaft or any shaft not directly connected with the fault, through a gear stage.

3.2.2 Measurements with magnetic encoders

The following results obtained with magnetic encoders have been chosen with a different operating rotation speed which is set to 2000 rpm in order to show high frequency conditions. When using a magnetic encoder, the angular location of pulses is less precise than with optical encoders and leads artifacts on angular spectral analysis of instantaneous angular speed. In Figure 9, the spectra for the three fault conditions are contaminated with integer order harmonics by the magnetic encoder.

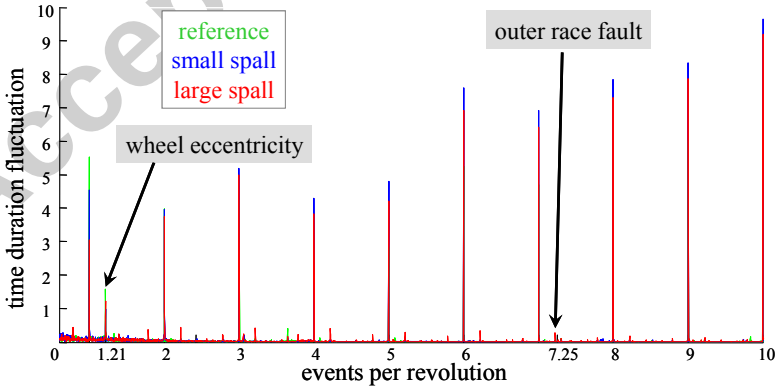

Figure 9: Instantaneous angular speed spectra of angular sampled signal of pulse time duration with magnetic encoder

In spite of these components, the wheel eccentricity component and the angular frequency channel attached to the outer race fault remain visible due to their non-integer location. Correction of this contamination can be done by removing the signature of the encoder. This signature is obtained by performing a synchronous average of the signal with a window length equal to one revolution and then

restoring a signal by duplicating this averaged revolution over the length of initial signal. The result of this filtering is presented in Figure 10 for the largest spall condition.

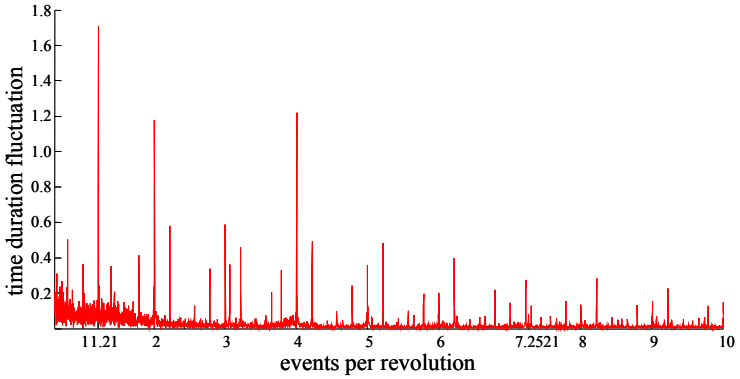

Figure 10: Instantaneous angular speed spectra of angular sampled signal after magnetic encoder signature cancellation

As in the previous section, the focused view of the spectral analysis arrives at the same conclusions concerning the 6th harmonic of acyclism and outer race fault and is shown in Figure 11. The relative difference between the levels obtained for the three conditions is always observed but less strongly for the small spall condition.

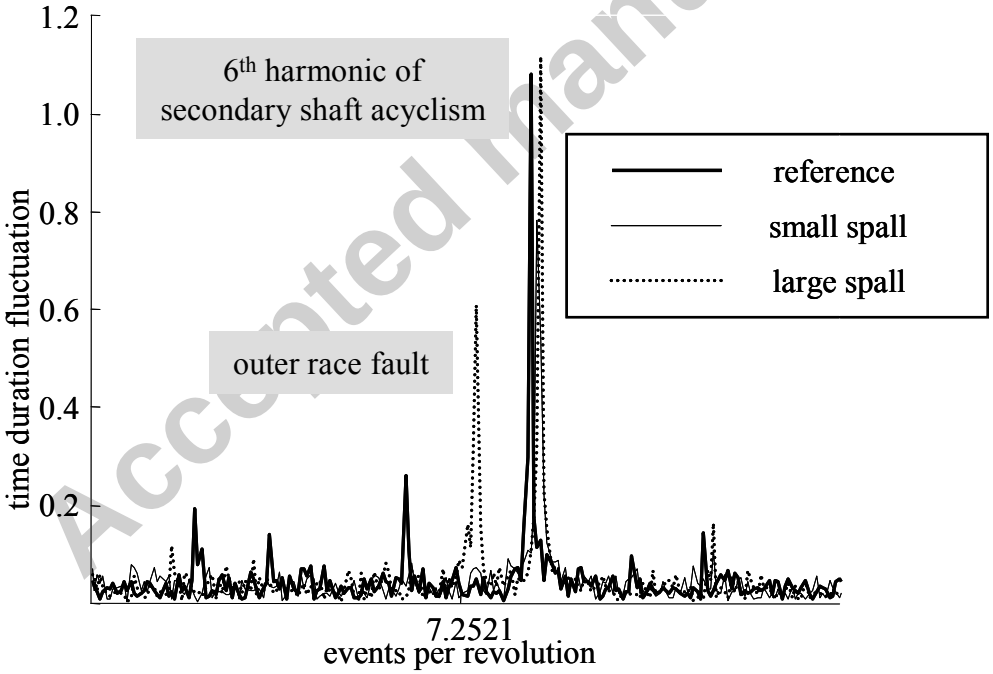

Figure 11: Extended view of the instantaneous speed spectra with magnetic encoder under different operating conditions (speed = 2000 rpm, torque = 60 Nm)

Compared to the previous optical encoder measurements, these conditions are representative of industrial conditions with robust transducers and especially with actual speed conditions.

3.3 Measurements with variable speed operating conditions

The most attractive property of angular sampling lies on its independence with respect to varying rotation speed. This section gathers the main results obtained under varying speed conditions. These variations are generated manually through the electrical motor control console and an example of the time history of such variations is given in Figure 12.

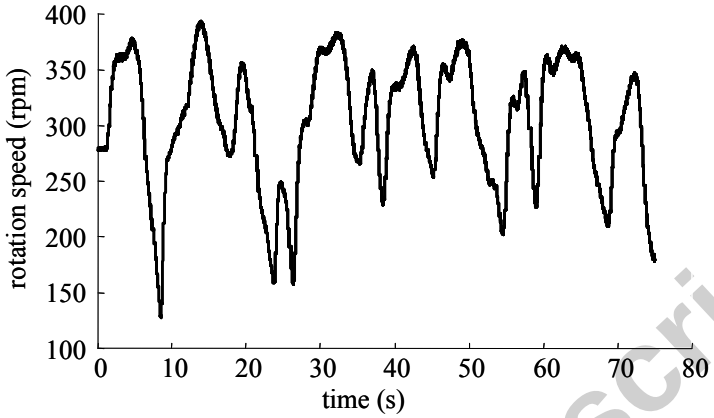

Figure 12: Generated rotation speed evolution during test measurements (torque = 20 Nm)

In this section, only the two largest faults have been investigated under low torque (20 Nm) both with optical and magnetic encoders. As shown in Figure 13 with the optical encoder, the spectral content is more chaotic in very low frequency range but frequency channels associated with the outer race spall and acyclism from the secondary shaft are always there and their levels are quite similar to those obtained in constant speed conditions.

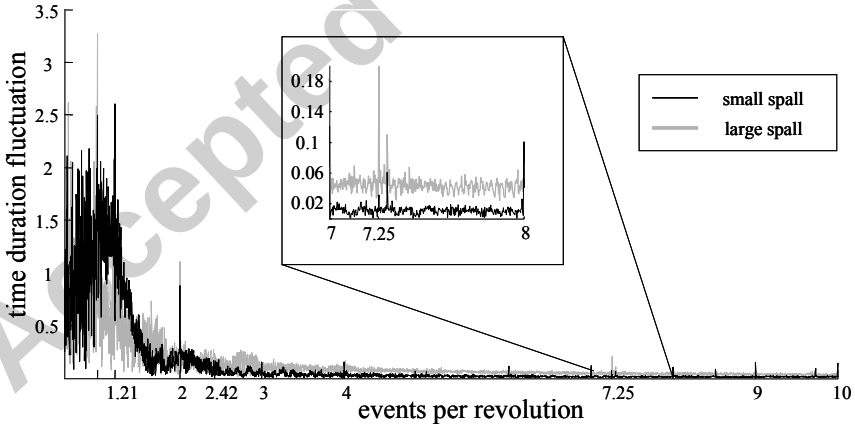

Figure 13: Instantaneous angular speed spectra of angular sampled signal with optical encoder under varying speed

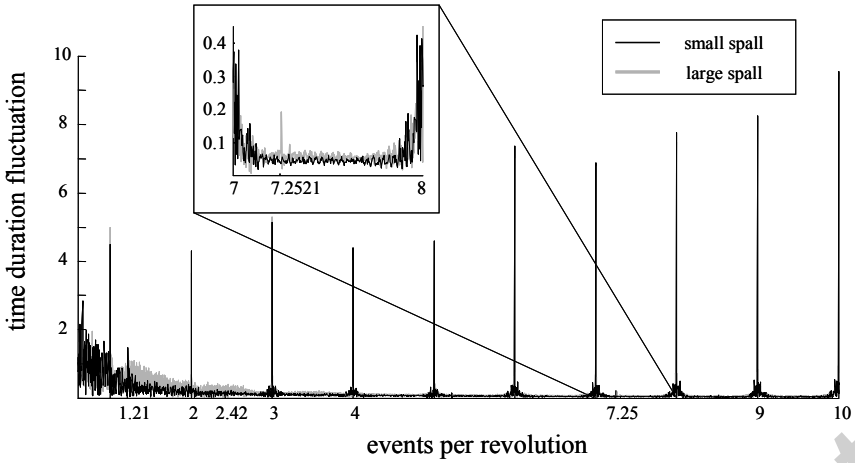

Figure 14: Instantaneous angular speed spectra of angular sampled signal with magnetic encoder under varying speed

With magnetic encoders, there are also perturbations in the low frequency range (see Figure 14). Even if no correction of encoder signature is performed, the spectral component of outer race fault exhibits a distinguishable level with spall on the outer race.

4 Experimental results on automotive wheels in real operating conditions

Another set of experiments have been performed on a small industrial vehicle in order to validate the feasibility of fault detection on a wheel bearing using magnetic encoding facilities implemented for anti blocking or trajectory control systems.

4.1 Description of the measurement device and operating conditions

The vehicle used for testing detection in an actual application is a small truck with a rear-wheel drive (see Figure 15) on which the front wheels are equipped with specific active sensors. A simple notch has been machined on the existing axle for positioning the sensor beside the magnetic target on the rotating part of the bearing. A tri-axial accelerometer is also mounted on the axle but is no more used in this study (see Figure 15). The bearing is a double row tapered roller bearing from NTN Corporation with a magnetic pattern offering a raw resolution of 60 pairs of poles. The sensor allows an interpolation factor of 40, leading to a global resolution for the magnetic encoder of 2400 pulses per revolution. The bearing change operation is performed traditionally without any change in the guidelines or any particular care. It must be remarked that, in this automotive application, the outer race is the rotating part of the bearing and inner race is fixed.

(a) vehicle for automotive tests

(b) bearing with its magnetic track

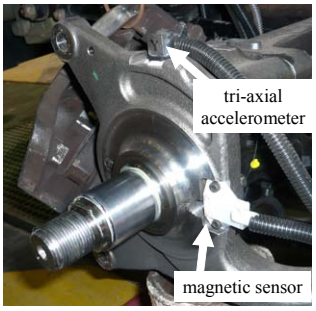

(c) detail of sensor location on each front axle

Figure 15: Views of the vehicle under test and sensor location

Different kinds of fault have been tested, from early stage of pitting to large and spread wear either on inner or outer races. As the bearing design is a double row, only the inner side of the bearing is subjected to pitting at different stages of evolution as shown in Figure 16. Thanks to NTN facilities, this pitting was obtained through a natural damage process.

(a) small spall on inner race (inner side)

(b) large spall on inner race (inner side)

(c) large spall on outer race (inner side)

Figure 16: Pictures of three different pitting faults (© NTN corp.)

The dimensions of the bearing give theoretical inner race frequency located at 11.39 events per revolution and theoretical outer race frequency located at 8.604 events per revolution. Faulty bearings can be mounted either on the left wheel axle or on the right wheel axle. Two load configurations of the vehicle (without load and full load) are systematically considered. Other operating conditions are summarized in the following list:

– constant speed of the vehicle (90 km/h), straight trajectory (acquisition length = 2.8 10^6 points),
– increasing and decreasing speed, straight trajectory (acquisition length = 2.8 10^6 points),
– constant speed (50 km/h), straight trajectory with bumps (acquisition length = 1.0 10^6 points),
– constant speed (50 km/h), clockwise turning (acquisition length = 0.75 10^6 points),
– constant speed (50 km/h), anticlockwise turning (acquisition length = 0.75 10^6 points),
– during bearing change, manual rotation of the wheel (acquisition length = 0.25 10^6 points).

Signal processing comes down to an FFT applied on an integer number of revolutions corresponding to the number of acquired points. Only significant results obtained from the whole set of experiments are presented in the next section.

4.2 Results on bearings with localized faults

As a reference configuration, the first test was performed with a healthy bearing on the right wheel and the bearing with small spall on the inner race on the left wheel. As shown in Figure 17, the spectral analysis is very dense for low frequency range but with a very important contribution in the range of the inner race frequency, from 11.32 to 11.33 channels. This contribution over large range may be put down to slipping of rolling elements during the test. Indeed, the load sharing between the two rows of this bearing design

may explain this not well located contribution as load conditions are changing during the test, inducing changes in the kinematics of the faulty row of the bearing. This enlargement effect can be associated with the random spread of frequency and local changes in kinematics.

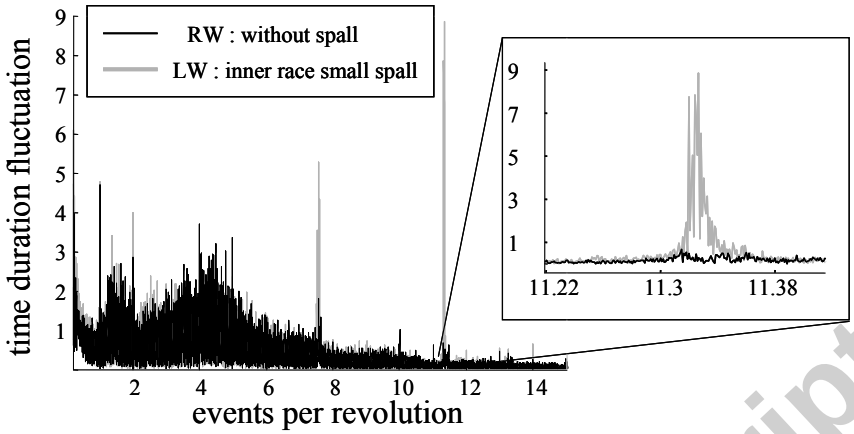

Figure 17: Inner race small spall detection (RW : Right Wheel, LW : Left Wheel)

The next configuration of interest is achieved by using the bearing with a large spall on the inner race on the left side. The two operating conditions involving a turning trajectory are presented in Figure 18. When anti clockwise turning is operated (see Figure 18 (a)), no fault contribution appears in frequency channels close to the inner race frequency (11.39 events per revolution) because the load applied on the bearing is fully supported by the outer side row of rolling elements.

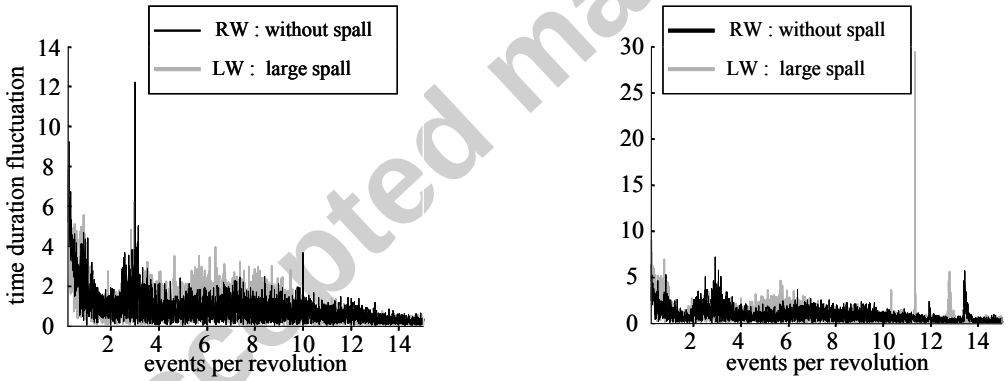

(a) anti clockwise turning steerage (b) clockwise turning steerage

Figure 18: Inner race large spall detection (RW : Right Wheel, LW : Left Wheel)

Conversely, when clockwise turning steerage occurs (see Figure 18 (b)), only the inner side row is supporting the load and the spall response is clearly seen at the right location, without the slip effect caused by load sharing as previously shown. These two tests performed without load on the truck allow also the validation that the weight of the truck is sufficient for fault detection on the inner race of the bearing. In Figure 18 (b), ones can notice that the same component appears on two different channels on the left or the right wheels. This is supposed to be a frequency contribution like acyclism from the motor, inducing small truck speed fluctuations. These fluctuations are then translated as angular contribution on each wheel with different rotation speed (the left wheel is running faster during clockwise turning steerage).

The last operating condition presented in this paper is performed with a large spall on the outer race of the left bearing without vehicle load during a straight trajectory at constant speed. In the particular case, the fault is alternatively loaded and unloaded during the revolution of the wheel, generating a modulation

effect. This is clearly shown in Figure 19 with activated channels in the spectrum at the fault frequency (8.604 events per revolution) and channels located on each side at a distance of one, two or three events per revolution. The small difference in frequency location (8.67 instead of 8.604) can be attributed to changes in kinematics due to dimension tolerances and/or to the applied load. Particularly in conical roller bearing, the axial position where there is no slip changes with permanent load and consecutive deformations, therefore leading to permanent kinematic changes in the bearing.

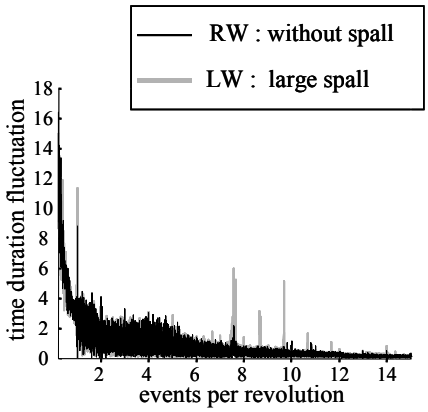

(a) instantaneous angular speed spectra of angular sampled signal

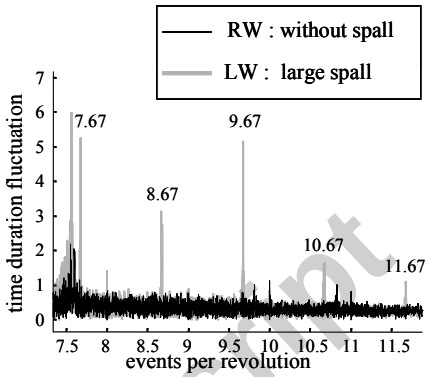

(b) effect of modulation due to spall location

Figure 19: Outer race large spall detection with modulation effect (RW : Right Wheel, LW : Left Wheel)

This well known modulation effect does not induce a random slipping effect with the spread of contribution over neighboring channels like in Figure 17. The contribution located at 7.55 events per revolution is supposed to be a consequence of motor contribution like previously submitted.

Many more other configurations have been tested but not reported in this paper, contributing to the general conclusions given and to the firm and robust feeling that instantaneous angular speed measurement is a very promising tool for early fault detection in bearings.

5 Conclusions

The main objective of this paper lies on the proof that instantaneous angular speed measurement with a true angular sampling is a very promising key feature in detecting bearing faults early in their damage process. This measurement is based upon classical through-shaft encoders with magnetic or optical gratings now available in industrial packages. The instantaneous angular speed measurement principle takes advantage of the Pulse Timing Method and is based on the kinematics of the device under monitoring. It only requires counter/timer devices and a high frequency clock (80 MHz).

This study, mainly supported by experimental results, proves that instantaneous angular speed exhibits small fluctuations with periodic components well located in the angular frequency domain when spalling appears. This novel indicator is also proved to be efficient for different kinds of early fault detection in bearings and to be robust for actual operating conditions. Firstly, measurements have been carried out on an automotive gearbox equipped with both optical and magnetic encoders and with one bearing offering three levels of early spalling on its outer race. In a second validation step, only magnetic encoders have been used on the front wheels of a small industrial vehicle with double row tapered roller bearings. Different kinds of spalling damage have been analyzed for faults on the outer or inner races. A wide range of operating conditions have been tested for the two applications with varying speed, load, external excitations, gear ratio, etc.

As expected, optical encoders provide a higher quality signal compared to magnetic encoders which introduce noise components at integer orders of rotating shaft frequency. This signature does not affect the non-integer frequency channels associated with bearing faults and can be avoided by means of the angular averaging process. The tests performed, either with high magnitude changes in rotating speed for the automotive gearbox or with different operating conditions in the case of vehicle wheels, also establish the robustness of the proposed methodology.

Even if the proposed measurement requires a high resolution spectrum only available through angular sampling, the post-processing consists in a classical and simple Fourier transform. For similar post-processing conditions, angular frequency channels kinematically related to the fault periodicity show significant magnitude differences related to the damage size. Sideband effects are evidently seen when the fault is located on rotating parts of the bearing due to load modulation. Additionally, slip effects are also suspected to be at the origin of widening of spectrum peaks in the case of double row bearings loaded in a pure radial direction.

Further work remains in order to investigate the relationship between the magnitude of bearing components and the damage progress. Moreover, the changes induced by different gear ratios on the automotive application awaken an interest in comparing different operating kinematics.

Acknowledgements

This study was supported by Rhône-Alpes Regional Council in the framework of DIAGeROS project. The authors are deeply grateful to NTN Corp. and SNR for providing faulty bearings and Volvo 3P for test facilities. They also would like to thank all the contributing persons for their technical support and valuable experience, particularly Y. Hiltcher (LaMCoS), G. Dejean (Volvo 3P), J. Couvert (Ipsys for Volvo 3P), P. Desbiolles (SNR), M. El Badaoui and F. Guillet (LASPI) and N. Penet (INSAVALOR).

References

[1] P. D. Samuel and D. J. Pines, "A review of vibration-based techniques for helicopter transmission diagnostics," *Journal of Sound and Vibration*, vol. 282, pp. 475–508, Apr. 2005.

[2] C. J. Stander, P. S. Heyns, and W. Schoombie, "Using vibration monitoring for local fault detection on gears operating under fluctuating load conditions," *Mechanical Systems and Signal Processing*, vol. 16, pp. 1005–1024, Nov. 2002.

[3] R. B. Randall, "New method of modeling gear faults," *American Society of Mechanical Engineers (Paper)*, pp. 9–, 1981.

[4] N. Sawalhi and R. Randall, "Simulating gear and bearing interactions in the presence of faults: Part i. the combined gear bearing dynamic model and the simulation of localised bearing faults," *Mechanical Systems and Signal Processing*, vol. 22, pp. 1924–1951, Nov. 2008.

[5] F. Bonnardot, M. El Badaoui, R. Randall, J. Danière, and F. Guillet, "Use of the acceleration signal of a gearbox in order to perform angular resampling (with limited speed fluctuation)," *Mechanical Systems and Signal Processing*, vol. 19, pp. 766–785, July 2005.

[6] S. Braun and B. Seth, "On the extraction and filtering of signals acquired from rotating machines," *Journal of Sound and Vibration*, vol. 65, pp. 37–50, July 1979.

[7] F. Bonnardot, R. Randall, and J. Antoni, "Unsupervised angular resampling and noise cancellation for planetary bearing fault diagnosis," *International Journal of Acoustics and Vibrations*, vol. 9, no. 2, 2004.

[8] J. Antoni, J. Daniere, and F. Guillet, "Effective vibration analysis of ic engines using cyclostationnarity. part i.a methodology for condition monitoring," *Journal of Sound and Vibration*, vol. 257, pp. 815–837, Nov. 2002.

[9] X. Kong, *Gear train monitoring by transmission error method*. PhD thesis, University of Wisconsin-Madison, 1987.

[10] J. Mahfoudh and D. Rémond, "Experimental study of the transmission error for the detection of gear faults," in *American Society of Mechanical Engineers, International Gas Turbine Institute, Turbo Expo (Publication) IGTI*, vol. 1, (Atlanta, GA, United States), pp. 345–349, American Society of Mechanical Engineers, New York, NY 10016-5990, United States, 2003.

[11] D. Rémond and J. Mahfoudh, "From transmission error measurements to angular sampling in rotating machines with discrete geometry," *Shock and Vibration*, vol. 12, no. 2, pp. 149–161, 2005.

[12] D. Rémond, "Practical performances of high-speed measurement of gear transmission error or torsional vibrations with optical encoders," *Measurement Science & Technology*, vol. 9, no. 3, pp. 347–353, 1998.

[13] P. J. Loughlin and B. Tacer, "Instantaneous frequency and the conditional mean frequency of a signal," *Signal Processing*, vol. 60, pp. 153–162, July 1997.

[14] K. R. Fyfe and E. D. S. Munck, "Aanalysis of computed order tracking," *Mechanical Systems and Signal Processing*, vol. 11, pp. 187–205, Mar. 1997.

[15] C. Stander and P. Heyns, "Instantaneous angular speed monitoring of gearboxes under non-cyclic stationary load conditions," *Mechanical Systems and Signal Processing*, vol. 19, pp. 817–835, July 2005.

[16] J. Yang, L. Pu, Z. Wang, Y. Zhou, and X. Yan, "Fault detection in a diesel engine by analysing the instantaneous angular speed," *Mechanical Systems and Signal Processing*, vol. 15, pp. 549–564, May 2001.

[17] F. Gu, I. Yesilyurt, Y. Li, G. Harris, and A. Ball, "An investigation of the effects of measurement noise in the use of instantaneous angular speed for machine diagnosis," *Mechanical Systems and Signal Processing*, vol. 20, pp. 1444–1460, Aug. 2006.